

ALMA observations of molecular gas in the host galaxy of AT2018cow

KANA MOROKUMA-MATSUI,^{1,*} TOMOKI MOROKUMA,¹ NOZOMU TOMINAGA,² BUNYO HATSUKADE,¹ MASAO HAYASHI,³
YOICHI TAMURA,⁴ YUICHI MATSUDA,^{3,5} KAZUHITO MOTOGI,⁶ KOTARO NIINUMA,⁶ AND MASAHIRO KONISHI¹

¹*Institute of Astronomy, Graduate School of Science, The University of Tokyo, 2-21-1 Osawa, Mitaka, Tokyo 181-0015, Japan*

²*Department of Physics, Faculty of Science and Engineering, Konan University, 8-9-1 Okamoto, Kobe, Hyogo 658-8501, Japan*

³*National Astronomical Observatory of Japan, 2-21-1 Osawa, Mitaka, Tokyo 181-8588, Japan*

⁴*Department of Physics, Nagoya University, Furo-cho, Chikusa-ku, Nagoya 464-8602, Japan*

⁵*Graduate University for Advanced Studies (SOKENDAI), Osawa 2-21-1, Mitaka, Tokyo 181-8588*

⁶*Graduate School of Sciences and Technology for Innovation, Yamaguchi University, Yoshida 1677-1, Yamaguchi, Yamaguchi 753-8512, Japan*

(Received –; Revised –; Accepted –)

Submitted to ApJL

ABSTRACT

We investigate the molecular gas in, and star-formation properties of, the host galaxy (CGCG 137-068) of a mysterious transient, AT2018cow, at kpc and larger scales, using archival band-3 data from the Atacama Large Millimeter/submillimeter Array (ALMA). AT2018cow is the nearest Fast-Evolving Luminous Transient (FELT), and this is the very first study unveiling molecular-gas properties of FELTs. The achieved rms and beam size are 0.21 mJy beam⁻¹ at a velocity resolution of 40 km s⁻¹ and 3''.66 × 2''.71 (1.1 kpc × 0.8 kpc), respectively. CO(*J*=1-0) emission is successfully detected. The total molecular gas mass inferred from the CO data is (1.85 ± 0.04) × 10⁸ M_⊙ with the Milky Way CO-to-H₂ conversion factor. The H₂ column density at the AT2018cow site is estimated to be 8.6 × 10²⁰ cm⁻². The ALMA data reveal that (1) CGCG 137-068 is a normal star-forming (SF) dwarf galaxy in terms of its molecular gas and star-formation properties and (2) AT2018cow is located between a CO peak and a blue star cluster. These properties suggest on-going star formation and favor the explosion of a massive star as the progenitor of AT2018cow. We also find that CGCG 137-068 has a solar or super-solar metallicity. If the metallicity of the other FELT hosts is not higher than average, then some property of SF dwarf galaxies other than metallicity may be related to FELTs.

Keywords: galaxies: ISM — galaxies: individual (CGCG 137-068) — supernovae: general — ISM: molecules

1. INTRODUCTION

Recent high-cadence and wide-field surveys have discovered a new class of objects: Fast-Evolving Luminous Transients (FELT, e.g., [Drout et al. 2014](#); [Rest et al. 2018](#); [Tominaga et al. submitted](#)), providing various observed properties such as light curves, spectral energy distributions and environments. The properties of FELTs which distinguish them from other classes of transients are their featureless spectra and quickly de-

clining light curves ($t_{1/2} \sim$ several days). AT2018cow is one of the FELTs, but its close proximity (60 Mpc) provides us a unique opportunity to study in detail physical properties of a FELT for the first time. It was discovered by the ATLAS survey on June 16, 2018, in the disk of dwarf star-forming (SF) galaxy, CGCG 137-068 ([Prentice et al. 2018](#)), and since that time it has been monitored at various wavelengths from radio to γ -ray (e.g., [Margutti et al. 2019](#); [Ho et al. 2019](#); [Perley et al. 2019](#)). It is characterized by a rapid rise time in brightness (a few days), a blue spectrum ($\sim 30,000$ K), high optical luminosity (4×10^{44} erg s⁻¹), initially featureless optical spectra, no γ -ray flash, high radio luminosity, and long-lived mm-wavelength emission ([Prentice et al. 2018](#);

Corresponding author: Kana Morokuma-Matsui
kanamoro@ioa.s.u-tokyo.ac.jp

* JSPS Fellow

Margutti et al. 2019; Ho et al. 2019; Perley et al. 2019; Kuin et al. 2019). With these observational constraints, various scenarios for the event have been proposed, and are roughly classified into two groups: massive star explosions (Perley et al. 2019; Margutti et al. 2019), and tidal disruption events (TDEs) in which a white dwarf is torn apart by an intermediate-mass black hole (Kuin et al. 2019; Perley et al. 2019).

Insight into the nature of transients is provided not only by observing the objects themselves but also their host galaxies, especially in order to distinguish whether events are related to the deaths of massive stars (i.e., on-going star formation) or not. Roychowdhury et al. (2019) found that AT2018cow resides in a ring-like HI structure seen in ~ 6 -arcsec resolution data taken with the Giant Metrewave Radio Telescope (GMRT). They concluded that the HI data indicates a massive-star scenario for AT2018cow, since such a ring is an ideal site for active star formation. In contrast, Michałowski et al. (2019) reported an absence of atomic gas at the AT2018cow site with a ~ 14 -arcsec beam, and claimed that a TDE is a more plausible scenario for the progenitor of AT2018cow based on their GMRT observations. The cold gas properties of the AT2018cow site are still controversial, and it is important to investigate it using molecular gas, the raw material of star formation.

In this paper, we study the molecular-gas and star-formation properties of CGCG 137-068 and local AT2018cow site using CO($J=1-0$) data taken with the Atacama Large Millimeter/submillimeter Array (ALMA). We adopt a distance to CGCG 137-068 of 60 Mpc ($1'' \sim 291$ pc) and cosmology parameters of $(h, \Omega_M, \Omega_\Lambda) = (0.7, 0.3, 0.7)$ throughout the paper.

2. DATA AND ANALYSIS

ALMA band-3 Time-Division-Modes (TDM) data were obtained on June 30 and July 16, 2018, with an antenna configuration of C43-1 in a target-of-opportunity (ToO) observation (project code of 2017.A.00045.T, PI: Steve Schulze). Antenna baselines range from 15 m to 161 m, and a maximum recoverable scale is 29 arcsec or 8.4 kpc. Since the original purpose of this observation is to measure the continuum flux of AT2018cow at band 3 (100.00 – 115.99 GHz), the data are taken in TDM mode, i.e., a frequency resolution of 15.625 MHz, corresponding to a velocity resolution of 40.64 km s⁻¹ at the observing frequency. The on-source integration time of each execution was 19.7 min. The CO($J=1-0$) emission line (rest frequency ν_{rest} of 115.271202 GHz) was covered in one of the upper-sideband spectral windows (a CO spectrum is shown in Figure 1).

Data calibration and imaging were conducted with the standard ALMA data analysis package, the Common Astronomy Software Applications (CASA, McMullin et al. 2007; Petry & CASA Development Team 2012). The absolute flux and gain fluctuations of the 12-m data were calibrated with the ALMA Science Pipeline (version of r40896 of Pipeline-CASA51-P2-B) in the CASA 5.1.1 package. The flux accuracy of the ALMA 12-m band-3 data is reported to be better than 5 % (ALMA proposer’s guide). Continuum emission is subtracted using the UVCONTSUB task and a ¹²CO($J=1-0$) mosaic data cube is generated with the TCLEAN task in CASA version 5.4 with options of Briggs weighting with a robust parameter of 0.5, auto-multithresh mask with standard values for 12-m array data provided in the CASA Guides for auto-masking¹ (sidelobethreshold of 2.0, noisethreshold of 4.25, minbeamfrac of 0.3, lownoisethreshold of 1.5, and negativethreshold of 15.0), and niter of 10000. The achieved synthesized beam is $3''.66 \times 2''.71$ (1.1 kpc \times 0.8 kpc at the distance of CGCG 137-068) with a P.A. of -27.8° . The achieved rms noise (σ_{rms}) is 0.21 mJy beam⁻¹ after primary beam correction at the velocity resolution of 40.64 km s⁻¹ in the box area centered on the galaxy center with a width and height of 25 arcsec in the emission-free channels (Figure 1b).

3. PROPERTIES OF AN CGCG 137-068

In this section, we present local-site (Section 3.1) and host-galaxy properties of AT2018cow derived with the ALMA data (Section 3.2).

3.1. 1-kpc-scale properties

Figure 1 shows ALMA CO($J=1-0$) moment maps and optical images obtained in the Sloan Digital Sky Survey (SDSS) of CGCG 137-068. The basic and derived parameters of AT2018cow site are summarized in Table 1. The ALMA data reveal that the AT2018cow is located at the edge of one of the CO peaks to the west of the galaxy center. The H₂ column density, $N(\text{H}_2)$, at the AT2018cow site is estimated to be 8.6×10^{20} cm⁻², using the standard CO-to-H₂ conversion factor from the Milky-Way of $X_{\text{CO}} = 2.0 \times 10^{20}$ cm⁻² (K km s⁻¹)⁻¹ (Bolatto et al. 2013)² since CGCG 137-068 has a solar or super-solar metallicity (see below). This corre-

¹ https://casaguides.nrao.edu/index.php/Automasking_Guide

² The conversion from Jy beam⁻¹ to Kelvin is done based on the Rayleigh-Jeans approximation with an equation of $T = 1.222 \times 10^6 \frac{I}{\nu^2 \theta_{\text{maj}} \theta_{\text{min}}}$, where T is the brightness temperature in Kelvin, ν is the observing frequency in GHz, θ_{maj} and θ_{min} are half-power beam widths along the major and minor axes in arcsec, respectively and I is the brightness in Jy beam⁻¹.

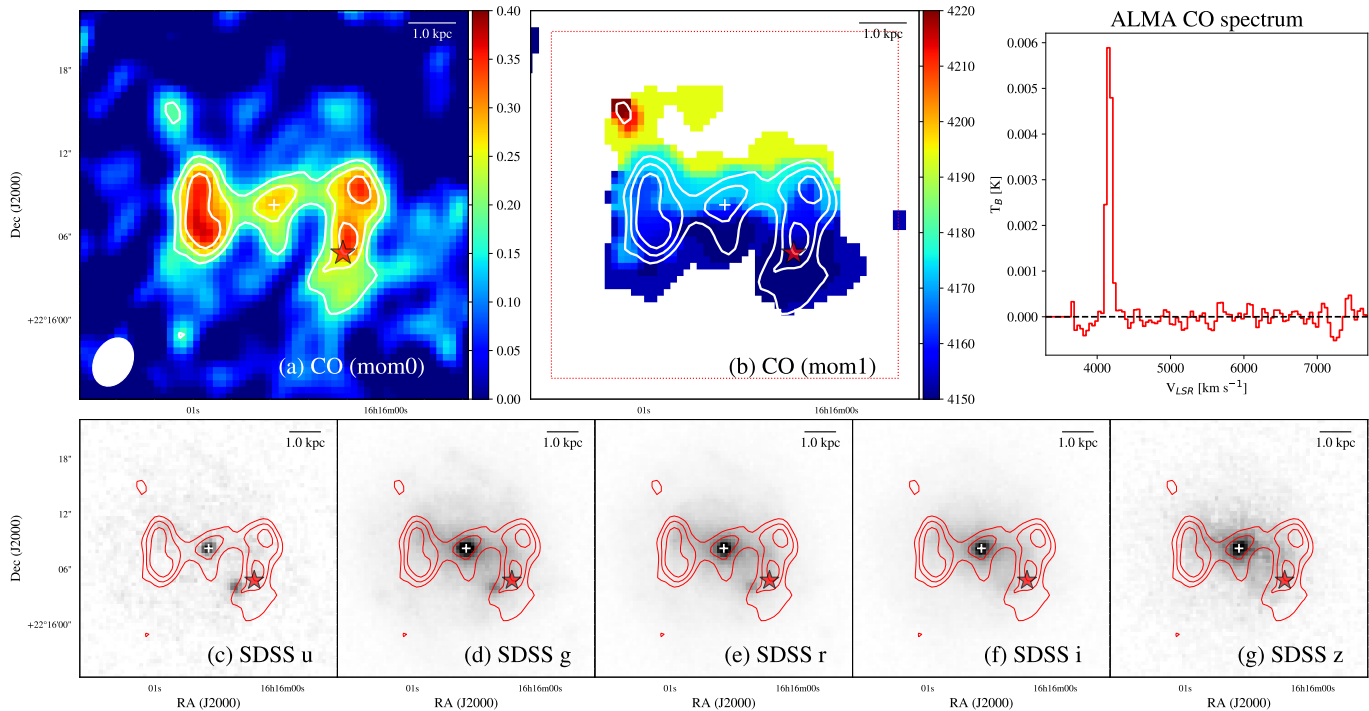


Figure 1. (a) ALMA CO($J=1-0$) integrated intensity map in units of $\text{Jy beam}^{-1} \text{ km s}^{-1}$ and (b) velocity field of CGCG 137-068 in units of km s^{-1} (“radio”-definition LSR velocity). SDSS optical images are also shown for a comparison: (c) u , (d) g , (e) r , (f) i , (g) z . Contours in each figure indicate the CO($J=1-0$) integrated intensity with contour levels of $(2.5, 3.5, 4.5) \times \sigma_{\text{rms,I.I.}}$, where $\sigma_{\text{rms,I.I.}}$ is $0.07 \text{ Jy beam}^{-1} \text{ km s}^{-1}$. Positions of the AT2018cow and galaxy center are indicated with a red star and a white cross, respectively. The ALMA beam ($3''.66 \times 2''.71$ with a position angle of -27.8°) is indicated as a white-filled circle at the bottom-left corner of the panel (a). The ALMA CO spectrum averaged over the area enclosed by red dotted line in the panel (b) is also shown at the upper right corner.

sponds to a molecular gas mass surface density, Σ_{mol} , of $14 \text{ M}_\odot \text{ pc}^{-2}$ (Figure 1). The CO velocity field is qualitatively consistent with the HI velocity field, showing a monotonic velocity increase from south to north. No disturbed velocity field is observed at the AT2018cow site with a velocity resolution of $\sim 40 \text{ km s}^{-1}$.

3.2. Galactic-scale properties

The properties related to molecular gas are presented in Table 1, together with other basic properties. The total molecular gas mass is estimated to be $(1.85 \pm 0.04) \times 10^8 \text{ M}_\odot$. Both the stellar mass (M_{star}) and star formation rate (SFR) values are taken from Perley et al. (2019), the gas-phase metallicity is measured from the SDSS spectrum, and the atomic gas mass (M_{atom}) is from Roychowdhury et al. (2019). The location of the host galaxy in the Baldwin, Phillips & Telervich (BPT) diagram suggests that it is a SF galaxy ($\log([\text{N II}]/\text{H}\alpha) = -0.35$, $\log([\text{O III}]/\text{H}\alpha) = -0.40$, $\log([\text{S II}]/\text{H}\alpha) = -0.43$, Baldwin et al. 1981). Note that the metallicities of CGCG 137-068 estimated with different calibrations are nearly solar or super-solar (cf., 8.69 for the Solar, Asplund et al. 2009): 8.96 (Tremonti

et al. 2004) with “MPA-JHU” calibration³; 9.35 (Zaritsky et al. 1994) and 8.98 (Pilyugin & Thuan 2005) with “ R_{23} ”; 8.77 (Denicoló et al. 2002) and 8.65 (Pettini & Pagel 2004) with “N2”; 8.71 with “O3N2” (Pettini & Pagel 2004).

In Figure 2, we compare the integrated galactic properties (SFR, metallicity, $M_{\text{atom}}/M_{\text{star}}$, $M_{\text{mol}}/M_{\text{star}}$, star formation efficiency of molecular gas (SFE(mol)), and $M_{\text{mol}}/M_{\text{atom}}$, as a function of M_{star}) of CGCG 137-068 with those of xGASS (Catinella et al. 2018) and xCOLD-GASS galaxies (Saintonge et al. 2017) at similar redshifts. Note that SFE(mol) of CGCG 137-068 is comparable to that of host galaxies of long-duration gamma-ray bursts (GRBs, e.g., Hatsukade et al. 2019), which are thought to be associated with the explosion of massive stars. Overall, CGCG 137-068 is a normal low-mass SF galaxy in terms of molecular-gas and star-formation properties, but has a relatively high metallicity considering its low stellar mass.

³ <https://wwwmpa.mpa-garching.mpg.de/SDSS/>

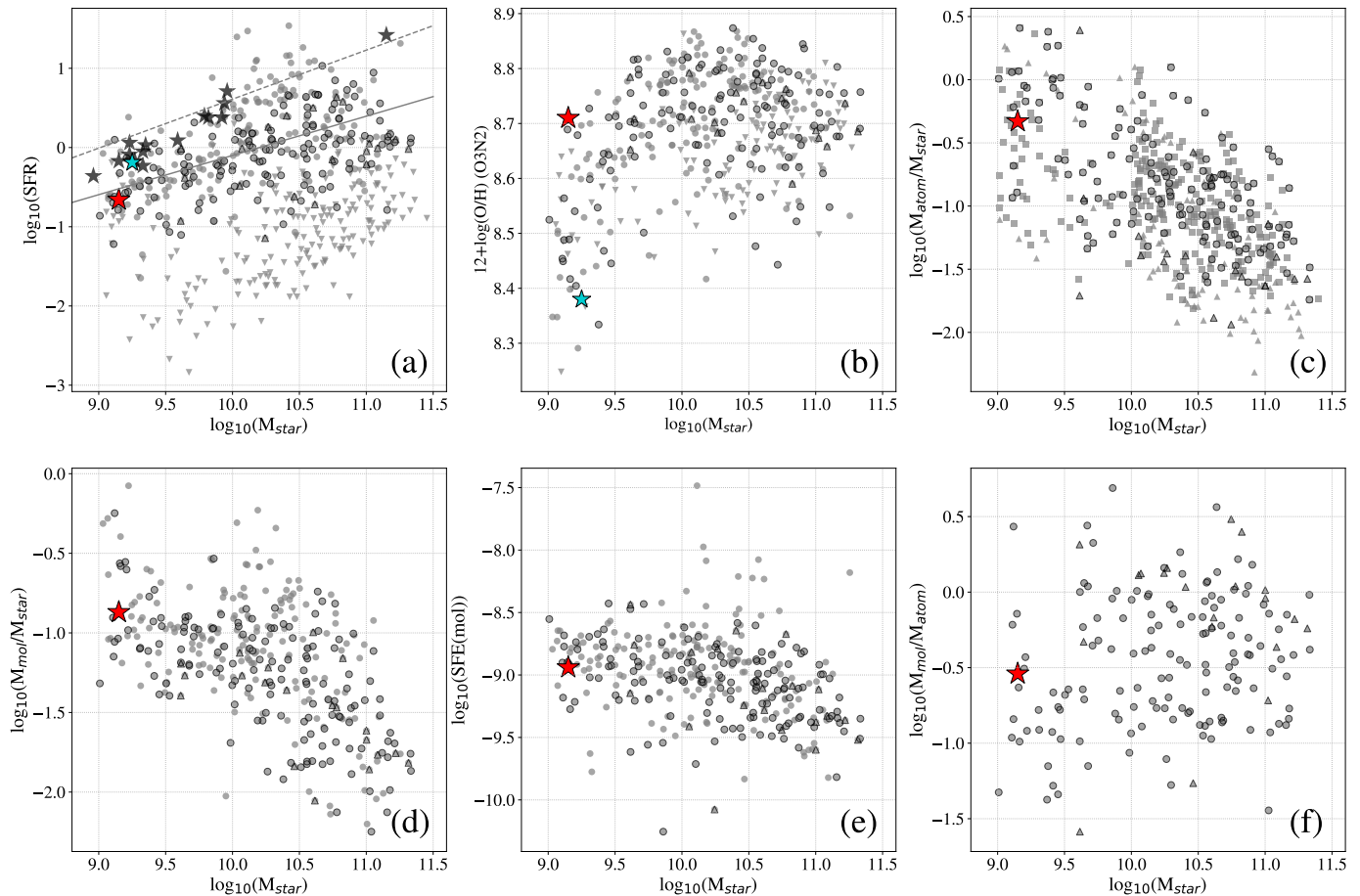


Figure 2. Basic properties of CGCG 137-068 (red-filled star, assuming IMF of Chabrier 2003) as a function of M_{star} : (a) $\log(\text{SFR})$, (b) Metallicity, $12 + \log(\text{O}/\text{H})$ (c) $\log(M_{\text{atom}}/M_{\text{star}})$ (d) $\log(M_{\text{mol}}/M_{\text{star}})$ (e) $\log(\text{SFE}(\text{mol})) = \log(\text{SFR}/M_{\text{mol}})$ (f) $\log(M_{\text{mol}}/M_{\text{atom}})$. For a reference, xCOLD GASS (Saintonge et al. 2017) and xGASS (Catinella et al. 2018) galaxies are plotted (grey-filled circle: CO detected, grey-filled down-pointing triangle: CO non-detected xCOLD GASS galaxies, grey-filled square: H I detected, grey-filled triangle: H I tentatively detected xGASS galaxies, black-open circle: both CO and H I detected, black-open triangle: CO detected and H I tentatively detected xCOLD GASS galaxies), assuming Chabrier (2003) IMF. Other FELTs (redshift of $0.12 < z < 1.56$, a median redshift of 0.485) from Pursiainen et al. (2018) also indicated as black-filled stars (not mentioned in the article but probably assuming IMF of Rana & Basu 1992). A FELT host in the Pursiainen et al. (2018) sample with SDSS spectrum is also plotted adopting MPA-JHU data (blue-filled star). SF main sequences at $z = 0.01414$ (a redshift of AT2018cow) and $z = 0.485$ (a median redshift of the other FELTs) are presented as grey solid and dashed lines, respectively (Speagle et al. 2014).

4. IMPLICATIONS FOR AT2018cow PROGENITOR

The ALMA data revealed that AT2018cow is located at the edge of one of the CO peaks to the west side of the galaxy center, and its host is a normal low-mass SF galaxy in terms of star-formation and cold-gas properties, except for its high metallicity. These properties of AT2018cow site and CGCG 137-068, i.e., abundant material for future star formation and proximity to a young star cluster, are suggestive of the progenitor scenarios featuring the explosion of a massive star. In this section, we first compare local-site and host-galaxy properties of AT2018cow with those of CCSNe and TDEs, then further compare with subclasses of CCSNe. The

comparison is summarized in Table 2. In addition, we also mention other FELTs, comparing the properties of their host galaxies to the properties of CGCG 137-068.

First, in terms of location within a host galaxy, core-collapse SNe (CCSNe) tend to reside in the outskirts of galaxies (Galbany et al. 2017), whereas TDEs are found generally at galactic centers (Komossa & Bade 1999; Gezari et al. 2012; Miller et al. 2015). AT2018cow is located at ~ 6 arcsec (1.75 kpc) from the galaxy center, which favors the CCSNe scenario. However, it should be noted that an off-center TDE event (12.5 kpc from center) was recently detected in X-rays in a large lentic-

Table 1. Basic properties of AT2018cow site and its host

Parameter	Value	Ref.
<i>Local site (AT2018cow)</i>		
R.A.	16 ^h 16 ^m 00 ^s .2242	1
Dec.	+22°16′04″.890	1
$R_{\text{AT2018cow}}^*$	6″.0 (1.75 kpc)	–
Σ_{mol} ($M_{\odot} \text{ pc}^{-2}$)	14	this study
$N(\text{H}_2)$ (cm^{-2})	8.6×10^{20}	this study
<i>Host galaxy (CGCG 137-068)</i>		
R.A.	16 ^h 16 ^m 00 ^s .57	SDSS
Dec.	+22°16′08″.24	SDSS
Redshift	0.0141	SDSS
Distance (Mpc)	60	2
M_{star} (M_{\odot})	$10^{9.15}$	2
SFR ($M_{\odot} \text{ yr}^{-1}$)	0.22	2
sSFR (yr^{-1})	1.56×10^{-10}	2
$12+\log(\text{O}/\text{H})_{\text{MPA-JHU}}$	8.96	SDSS
M_{atom} (M_{\odot})	$(6.6 \pm 0.9) \times 10^8$	3
I_{CO} (K km s^{-1})	0.575 ± 0.020	this study
L'_{CO} ($\text{K km s}^{-1} \text{ pc}^2$)	$(4.34 \pm 0.15) \times 10^7$	this study
$\text{FWHM}_{\text{CO}}^{***}$ (km s^{-1})	85.5	this study
M_{mol} (M_{\odot})	$(1.85 \pm 0.04) \times 10^8$	this study
SFE(mol) (yr^{-1})	1.2×10^{-9}	this study
SFE(gas)** (yr^{-1})	2.6×10^{-10}	this study
$M_{\text{atom}}/M_{\text{star}}$	0.47	3
$M_{\text{mol}}/M_{\text{star}}$	0.13	this study
$M_{\text{mol}}/M_{\text{atom}}$	0.29	this study

NOTE— *Galactocentric distance. **SFE(gas) = SFR/($M_{\text{atom}}+M_{\text{mol}}$). ***From Gaussian fitted curve. Ref. 1: Bietenholz et al. (2018), 2: Perley et al. (2019), 3: Roychowdhury et al. (2019)

ular galaxy (Lin et al. 2018). This event is considered to be a TDE by a few $10^4 M_{\odot}$ black hole.

Second, it is claimed that transients of different types may arise preferentially in certain types of galaxies. TDEs are claimed to reside primarily in quiescent Balmer-strong galaxies (i.e., post-starburst galaxies) unlike CGCG 137-068 (e.g., Arcavi et al. 2014; French et al. 2016). In addition, TDE hosts tend to have a LINER/Seyfert nucleus based on BPT diagnostics, similar to those in other quiescent Balmer-strong galaxies (French et al. 2017). Statistical studies of CCSNe host galaxies, on the other hand, show that the number ratio of Type-I (H-poor, Ib and Ic) to Type-II (H-rich) CCSNe is not a strong function of the Hubble type (Hakobyan et al. 2014), that the Type-I-to-Type-II CCSNe number ratio tends to be high for SF galaxies based on BPT diagnostics (Hakobyan et al. 2014), and that Type-I

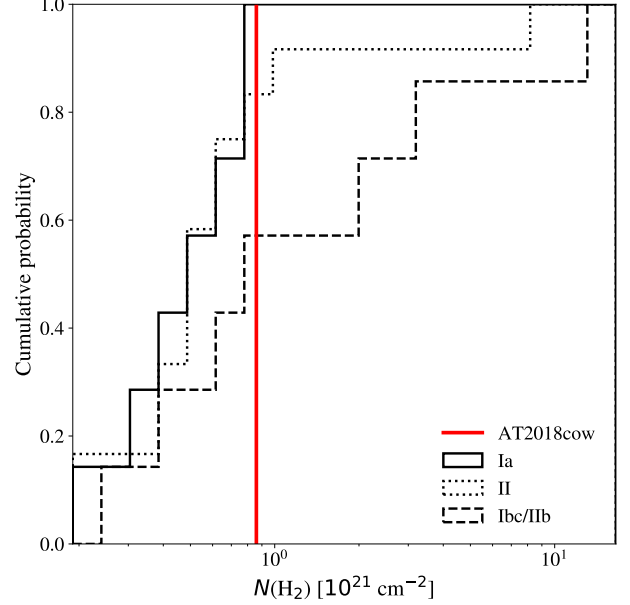


Figure 3. Comparison between H_2 column density at the AT2018cow site and that of other SNe sites from Galbany et al. (2017). Note that most of the SNe Ia and II data are upper limits.

CCSNe found in dwarf galaxies are either SNe Ib or broad-line SNe Ic (SNe Ic-BL), whereas normal SNe Ic dominate in giant galaxies (Arcavi et al. 2010). Thus, the galaxy type of CGCG 137-068 also suggests a CCSN scenario, especially SNe Ib or SNe Ic-BL.

Third, it is claimed that the kpc-scale $N(\text{H}_2)$ tends to be higher at Type-I CCSNe sites than Type-II CCSNe sites in nearby galaxies (Galbany et al. 2017). Compared to these SNe, $N(\text{H}_2)$ at the AT2018cow site is slightly higher than the Type-II CCSNe (mostly upper limits in the previous study), but comparable to Type-I CCSNe, which have a median of $N(\text{H}_2) \sim 9.4 \times 10^{20} \text{ cm}^{-2}$ (Figure 3). Note that HI emission is found to be not so strong or absent at the AT2018cow site (Roychowdhury et al. 2019; Michałowski et al. 2019). This is consistent with the previous studies on cold gas properties of nearby galaxies, where the dominant phase changes from atomic to molecular gas at $\Sigma_{\text{mol}} \sim 10 M_{\odot} \text{ pc}^{-2}$ (Bigiel et al. 2008).

Fourth, the association between CCSNe and HII regions is claimed to be different according to types of SNe: a higher association is found for Type-I CCSNe than Type-II CCSNe, suggesting that the progenitors of Type-I CCSNe are more massive than Type-II CCSNe (Anderson & James 2008; Crowther 2013). In the bottom of Figure 1, AT2018cow seems to be located between a u -band bright cluster and the molecular gas peak. The cluster tends to be brighter at shorter wave-

Table 2. Scoring table for progenitor models of AT2018cow

Scenario	<i>AT2018cow site</i>			<i>CGCG 137-068</i>			
	$R_{AT2018cow}$	$N(\text{H}_2)$	H II	BPT	SF activity	morphology	metallicity
TDEs	×	–	–	×	×	–	–
CCSNe SNe II	✓	×	Maybe ×	×	✓	✓	Maybe ×
SNe Ib	✓	✓	Maybe ✓	✓	✓	✓	Maybe ✓
SNe Ic	✓	✓	Maybe ✓	✓	✓	×	Maybe ✓
SNe Ic-BL w/ GRB	✓	✓	Maybe ✓	✓	✓	✓	×
SNe Ic-BL w/o GRB	✓	✓	Maybe ✓	✓	✓	✓	✓

lengths, suggesting it is young. The distance between the AT2018cow site and the cluster is 640 pc, which is much larger than the typical H II region but comparable to supergiant H II regions such as NGC 5461 of M 101 (a radius of ~ 500 pc, Crowther 2013). Although we do not have H α data, the proximity between the AT2018cow and the nearby young stellar cluster may suggest the AT2018cow site resembles local environments of Type-I CCSNe.

Finally, the high metallicity of CGCG 137-068 is one of its more noteworthy properties. Generally, it is reported that the metallicity at explosion sites is not a strong function of CCSNe types (Kuncarayakti et al. 2018), though the sites of Type-I SNe may have a slightly higher metallicity than those of Type-II SNe (Anderson et al. 2010). Some observations suggest that metallicity at the site of SNe Ic-BL without a long GRB tends to be higher than that of SNe Ic-BL with a long GRB (e.g., Modjaz et al. 2008; Japelj et al. 2018), although the sample size is small and the statistical significance is low (see also Modjaz et al. 2019). If the difference is real, these two populations are likely to be intrinsically different, possibly in terms of success or failure of break-out of a jet (Lazzati et al. 2012; Japelj et al. 2018). Considering that CGCG 137-068 was not accompanied by a GRB, the observed properties of CGCG 137-068 resemble those of SNe Ic-BL without a GRB.

In Figure 2a, we plot other FELTs listed as the “Gold sample”, i.e., most secure sample, with stellar mass and SFR estimations in Pursiainen et al. (2018). We can see that these host galaxies are also SF galaxies at their redshifts ($0.12 < z < 1.56$, a median redshift of 0.485)⁴ and tend to have low stellar mass ($8.26 < \log(M_{\text{star}}/M_{\odot}) < 11.15$, a median of 9.33), as CGCG 137-068. One of the FELT hosts in Pursiainen et al. (2018) without SFR estimation has SDSS spectroscopic data. In Figures 2a and b, we plotted this host using SDSS data, showing that

it is a low-mass SF galaxies with a relatively low metallicity. Meanwhile, some metallicity calibrations suggest that it has a super-solar metallicity⁵. This suggests that some properties of dwarf SF galaxies other than metallicity may be related to FELTs. However, the sample size ($N = 2$) is too small to conclude it and metallicity measurements of other FELT hosts are required.

5. SUMMARY

We investigate the molecular-gas and star-formation properties of the host galaxy (CGCG 137-068) and local site of AT2018cow using archival ALMA CO($J=1-0$) data. We found that:

1. AT2018cow is located between one of the CO peaks and a blue stellar cluster, both of which are indicators of on-going star formation.
2. The H₂ column density of the AT2018cow site is $8.6 \times 10^{20} \text{ cm}^{-2}$, which is slightly higher than that of Type-II CCSNe sites and comparable to that of Type-I CCSNe sites.
3. The total molecular gas mass is $(1.85 \pm 0.04) \times 10^8 M_{\odot}$, using a Milky-Way CO-to-H₂ conversion factor. With the literature data, $M_{\text{mol}}/M_{\text{star}}$, SFE(mol), and $M_{\text{mol}}/M_{\text{atom}}$ of CGCG 137-068 are 0.13, $1.2 \times 10^{-9} \text{ yr}^{-1}$, and 0.29, respectively.
4. Compared to reference galaxies at similar redshift (xGASS and xCOLD GASS galaxies), CGCG 137-068 is a normal SF dwarf galaxy in terms of SFR, $M_{\text{atom}}/M_{\text{star}}$, $M_{\text{mol}}/M_{\text{star}}$, SFE(mol), and $M_{\text{mol}}/M_{\text{atom}}$. The gas-phase metallicity of CGCG 137-068 is relatively high (solar or super-solar) for the stellar mass of CGCG 137-068.

⁴ The “SF main sequence” evolves with time (Speagle et al. 2014).

⁵ 8.60 (Tremonti et al. 2004) with “MPA-JHU” calibration; 8.82 (McGaugh 1991), 8.93 (Zaritsky et al. 1994) and 8.45 (Pilyugin & Thuan 2005) with “ R_{23} ”; 8.51 (Denicoló et al. 2002) and 8.36 (Pettini & Pagel 2004) with “N2”; 8.38 with “O3N2” (Pettini & Pagel 2004)

5. Compared to the previous studies on known transients, both the host-galaxy and local-site properties of the AT2018cow are indicative of massive-star explosions, especially SNe Ic-BL without GRB, although the observed properties of AT2018cow itself cannot be fully explained by SNe Ic-BL models.

For a more detailed understanding of AT2018cow, deep integral-field-spectroscopy observations of CGCG 137-068 are necessary to investigate the H α distribution and metallicity around the AT2018cow site, and to determine the age of the nearby young cluster. In addition, follow-up observations of the other FELT hosts, such as metallicity measurements, are required to place AT2018cow among the general population of FELT hosts. If the metallicity of the other FELT hosts is not higher than average, then some property of dwarf SF galaxies other than metallicity may be related to FELTs.

We are grateful to the anonymous referee for his/her helpful comments and to the PDJ collaboration for providing opportunities for fruitful discussions. KMM thank Dr. Yuu Niino for useful discussions. This study is supported by JSPS KAKENHI grant No.s of 15H02075, 15H00784, 16H02158, 17H06130, 17KK0098, 17H04831, 18H03721, and 19K03925. We also appreciate the kind help of Prof. Michael W. Richmond in improving the English grammar of the manuscript.

This paper makes use of the following ALMA data: ADS/JAO.ALMA#2017.A.00045.T. ALMA is a partnership of ESO (representing its member states), NSF (USA) and NINS (Japan), together with NRC (Canada), MOST and ASIAA (Taiwan), and KASI

(Republic of Korea), in cooperation with the Republic of Chile. The Joint ALMA Observatory is operated by ESO, AUI/NRAO and NAOJ.

Funding for the Sloan Digital Sky Survey IV has been provided by the Alfred P. Sloan Foundation, the U.S. Department of Energy Office of Science, and the Participating Institutions. SDSS-IV acknowledges support and resources from the Center for High-Performance Computing at the University of Utah. The SDSS web site is www.sdss.org.

SDSS-IV is managed by the Astrophysical Research Consortium for the Participating Institutions of the SDSS Collaboration including the Brazilian Participation Group, the Carnegie Institution for Science, Carnegie Mellon University, the Chilean Participation Group, the French Participation Group, Harvard-Smithsonian Center for Astrophysics, Instituto de Astrofísica de Canarias, The Johns Hopkins University, Kavli Institute for the Physics and Mathematics of the Universe (IPMU) / University of Tokyo, the Korean Participation Group, Lawrence Berkeley National Laboratory, Leibniz Institut für Astrophysik Potsdam (AIP), Max-Planck-Institut für Astronomie (MPIA Heidelberg), Max-Planck-Institut für Astrophysik (MPA Garching), Max-Planck-Institut für Extraterrestrische Physik (MPE), National Astronomical Observatories of China, New Mexico State University, New York University, University of Notre Dame, Observatório Nacional / MCTI, The Ohio State University, Pennsylvania State University, Shanghai Astronomical Observatory, United Kingdom Participation Group, Universidad Nacional Autónoma de México, University of Arizona, University of Colorado Boulder, University of Oxford, University of Portsmouth, University of Utah, University of Virginia, University of Washington, University of Wisconsin, Vanderbilt University, and Yale University.

REFERENCES

- Anderson, J. P., Covarrubias, R. A., James, P. A., Hamuy, M., & Haberman, S. M. 2010, *MNRAS*, 407, 2660
- Anderson, J. P., & James, P. A. 2008, *MNRAS*, 390, 1527
- Arcavi, I., Gal-Yam, A., Kasliwal, M. M., et al. 2010, *ApJ*, 721, 777
- Arcavi, I., Gal-Yam, A., Sullivan, M., et al. 2014, *ApJ*, 793, 38
- Asplund, M., Grevesse, N., Sauval, A. J., & Scott, P. 2009, *ARA&A*, 47, 481
- Baldwin, J. A., Phillips, M. M., & Terlevich, R. 1981, *PASP*, 93, 5
- Bietenholz, M., Margutti, R., Alexander, K., et al. 2018, *The Astronomer's Telegram*, 11900
- Bigiel, F., Leroy, A., Walter, F., et al. 2008, *AJ*, 136, 2846
- Bolatto, A. D., Wolfire, M., & Leroy, A. K. 2013, *ARA&A*, 51, 207
- Catinella, B., Saintonge, A., Janowiecki, S., et al. 2018, *MNRAS*, 476, 875
- Chabrier, G. 2003, *PASP*, 115, 763
- Crowther, P. A. 2013, *MNRAS*, 428, 1927
- Denicoló, G., Terlevich, R., & Terlevich, E. 2002, *MNRAS*, 330, 69
- Drout, M. R., Chornock, R., Soderberg, A. M., et al. 2014, *ApJ*, 794, 23
- French, K. D., Arcavi, I., & Zabludoff, A. 2016, *ApJL*, 818, L21

- . 2017, *ApJ*, 835, 176
- Galbany, L., Mora, L., González-Gaitán, S., et al. 2017, *MNRAS*, 468, 628
- Gezari, S., Chornock, R., Rest, A., et al. 2012, *Nature*, 485, 217
- Hakobyan, A. A., Nazaryan, T. A., Adibekyan, V. Z., et al. 2014, *MNRAS*, 444, 2428
- Hatsukade, B., Hashimoto, T., Kohno, K., et al. 2019, *ApJ*, 876, 91
- Ho, A. Y. Q., Phinney, E. S., Ravi, V., et al. 2019, *ApJ*, 871, 73
- Japelj, J., Vergani, S. D., Salvaterra, R., et al. 2018, *A&A*, 617, A105
- Komossa, S., & Bade, N. 1999, *A&A*, 343, 775
- Kuin, N. P. M., Wu, K., Oates, S., et al. 2019, *MNRAS*, arXiv:1808.08492
- Kuncarayakti, H., Anderson, J. P., Galbany, L., et al. 2018, *A&A*, 613, A35
- Lazzati, D., Morsony, B. J., Blackwell, C. H., & Begelman, M. C. 2012, *ApJ*, 750, 68
- Lin, D., Strader, J., Carrasco, E. R., et al. 2018, *Nature Astronomy*, 2, 656
- Margutti, R., Metzger, B. D., Chornock, R., et al. 2019, *ApJ*, 872, 18
- McGaugh, S. S. 1991, *ApJ*, 380, 140
- McMullin, J. P., Waters, B., Schiebel, D., Young, W., & Golap, K. 2007, in *Astronomical Society of the Pacific Conference Series*, Vol. 376, *Astronomical Data Analysis Software and Systems XVI*, ed. R. A. Shaw, F. Hill, & D. J. Bell, 127
- Michałowski, M. J., Kamphuis, P., Hjorth, J., et al. 2019, arXiv e-prints, arXiv:1902.10144
- Miller, J. M., Kaastra, J. S., Miller, M. C., et al. 2015, *Nature*, 526, 542
- Modjaz, M., Kewley, L., Kirshner, R. P., et al. 2008, *AJ*, 135, 1136
- Modjaz, M., Bianco, F. B., Siwek, M., et al. 2019, arXiv e-prints, arXiv:1901.00872
- Perley, D. A., Mazzali, P. A., Yan, L., et al. 2019, *MNRAS*, 484, 1031
- Petry, D., & CASA Development Team. 2012, in *Astronomical Society of the Pacific Conference Series*, Vol. 461, *Astronomical Data Analysis Software and Systems XXI*, ed. P. Ballester, D. Egret, & N. P. F. Lorente, 849
- Pettini, M., & Pagel, B. E. J. 2004, *MNRAS*, 348, L59
- Pilyugin, L. S., & Thuan, T. X. 2005, *ApJ*, 631, 231
- Prentice, S. J., Maguire, K., Smartt, S. J., et al. 2018, *ApJL*, 865, L3
- Pursiainen, M., Childress, M., Smith, M., et al. 2018, *MNRAS*, 481, 894
- Rana, N. C., & Basu, S. 1992, *A&A*, 265, 499
- Rest, A., Garnavich, P. M., Khatami, D., et al. 2018, *Nature Astronomy*, 2, 307
- Roychowdhury, S., Arabsalmani, M., & Kanekar, N. 2019, *MNRAS*, 485, L93
- Saintonge, A., Catinella, B., Tacconi, L. J., et al. 2017, *ApJS*, 233, 22
- Speagle, J. S., Steinhardt, C. L., Capak, P. L., & Silverman, J. D. 2014, *ApJS*, 214, 15
- Tremonti, C. A., Heckman, T. M., Kauffmann, G., et al. 2004, *ApJ*, 613, 898
- Zaritsky, D., Kennicutt, Jr., R. C., & Huchra, J. P. 1994, *ApJ*, 420, 87